

JOURNAL OF THE AMERICAN CHEMICAL SOCIETY

Theoretical X-ray Absorption Fine Structure Standards

J. J. Rehr,^{*,†} J. Mustre de Leon,^{†,‡} S. I. Zabinsky,[†] and R. C. Albers[§]

Contribution from the Department of Physics, FM-15, University of Washington, Seattle, Washington 98195, and Theoretical Division, Los Alamos National Laboratory, Los Alamos, New Mexico 87545. Received November 13, 1990

Abstract: Theoretical X-ray absorption fine structure (XAFS) standards are developed for arbitrary pairs of atoms throughout the periodic table ($Z \leq 94$). These standard XAFS spectra are obtained from *ab initio* single-scattering XAFS calculations, using an automated code, FEFF, which takes into account the most important features in current theories: (i) an exact treatment of curved-wave effects; (ii) approximate molecular potentials derived from relativistic atoms, (iii) a complex, energy-dependent self-energy; (iv) a well defined energy reference. FEFF also yields tables of XAFS phases and amplitudes as well as mean-free paths. Sample results are presented and compared with experimental results and with earlier work. We find that these theoretical standards are competitive with experimental standards, permitting XAFS analysis at lower wavenumbers and yielding distance determinations typically better than 0.02 Å and coordination numbers typically better than 20%. These standards also provide theoretical tests of chemical transferability in XAFS.

I. Introduction

X-ray absorption fine structure (XAFS), i.e., the oscillatory structure in the X-ray absorption coefficient, contains much quantitative information concerning the local structure near an absorbing atom.¹ This includes near-neighbor distances, coordination numbers, and structural and vibrational disorder in bond distances. Extracting this information with precision, however, requires a comparison with an accurately known reference system or "standard", either experimental or theoretical. Theoretical standards have usually been less successful than experimental standards, primarily because of approximations introduced into the calculations, rather than inadequacies of the fundamental theory.

Present theoretical standards include tables of XAFS phases and amplitudes^{2,3} and computer codes such as EXCURV.⁴ Each of these standards has its drawbacks: The tables of Teo and Lee² are based on a remarkably sophisticated theory⁵ that takes into account inelastic losses and self-energy effects; however, since these tabulations are intended for the EXAFS region, curved-wave corrections are approximated by an inner potential shift. The

tables of McKale et al.³ and EXCURV⁴ take curved-wave effects into account but are based on ground-state potentials and thus ignore the electron self-energy. All of these standards use as a free parameter the energy reference or "inner potential" E_0 . Since such ad hoc parameters compensate for other errors in the theory, such as an incorrect self-energy, they need have no direct physical interpretation. Another limitation of the above standards is the reliance on chemical transferability; they are based on a well-chosen potential, but system-dependent chemical effects are neglected. Moreover, other XAFS parameters, such as mean-free paths and core-hole lifetimes, must be added by hand.

Our goal in this work is to develop new XAFS standards based on a more complete theoretical model that removes the drawbacks mentioned above and reduces as much as possible the need for nonphysical fitting parameters. A second goal is to extend the range of validity of the theory to lower energies, thereby improving

(1) See, for example: *X-ray Absorption: Principles, Applications, Techniques of EXAFS, SEXAFS and XANES*; Prins, R., Köningsberger, D., Eds.; Wiley: New York, 1988.

(2) Teo, B.-K.; Lee, P. A. *J. Am. Chem. Soc.* **1979**, *101*, 2815.

(3) McKale, A. G.; Veal, B. W.; Paulikas, A. P.; Chan, S.-K.; Knapp, G. *S. J. Am. Chem. Soc.* **1988**, *110*, 3763.

(4) Binsted, N.; Gurman, S. J.; Campbell, J. W. *EXCURV*; SERC Daresbury Laboratory: Daresbury, Warrington, U.K., 1986.

(5) Lee, P. A.; Beni, G. *Phys. Rev. B* **1977**, *15*, 2862.

[†]University of Washington.

[‡]Present address: Electronics Division, Los Alamos National Laboratory, Los Alamos, NM 87545.

[§]Theoretical Division, Los Alamos National Laboratory.

the utility of the XAFS technique. These goals are accomplished here by an efficient, automated code for *ab initio* single-scattering XAFS calculation. The complete code is termed FEFF for the central role of the effective, curved-wave scattering amplitude, $f_{\text{eff}}(\pi, k, R)$, in the theory.⁶ The efficiency of the code makes *ab initio standards* generally accessible for routine XAFS analysis. Such standards are of course essential when experimental standards are not available. In addition FEFF yields new tables of XAFS parameters, i.e., *tabulated standards* for all pairs of atoms in the periodic table with $Z \leq 94$. Many other *ab initio* codes exist for XAFS calculations;⁷⁻⁹ however, to the best of our knowledge, none of these are readily accessible to nonexperts. In this article we focus on a description of these new theoretical standards and only summarize the underlying theory. We believe this degree of detail should be adequate for those interested in applying these standards in XAFS analysis. Systematic trends in the backscattering amplitudes and phase shifts vs atomic number Z have been studied in detail in the compilation of Teo and Lee.² Since the trends are qualitatively similar for the new standards, we do not repeat them here. Instead, we illustrate in a few cases the differences between our standards and those previously published. A second article which focuses primarily on the theoretical considerations behind our approach will be presented elsewhere.¹⁰

The paper is organized as follows: In section II a summary of our theoretical model is presented. Section III describes the *ab initio* standards based on FEFF, together with several comparisons to experiment. In section IV the tabulated standards are discussed. Finally, section V contains a summary and the conclusions.

II. Theoretical Model

Model System. In this section we briefly describe the theoretical model upon which FEFF is based.¹⁰ We consider a simplified model system consisting of an absorbing atom of atomic number Z_c surrounded by N identical neighbors of atomic number Z at a distance R . The XAFS photoabsorption spectrum χ_i for any given core level, i.e., K , L_1 , L_{III} , etc., is then calculated by using current XAFS theory.^{11,12} The theory is based on a scattering-theoretic framework¹² that includes curved-wave effects,^{6,13} inelastic losses, both extrinsic and intrinsic,^{5,14-17} and several technical improvements to previous treatments.¹⁰ In the construction of the molecular potential, the N neighbor atoms are all assumed to have a coordination number N' . This model potential is an improvement on isolated atomic potentials in that the local coordination is taken into account. The model system may not be accurate in cases where there are several atomic species; however, it is still adequate for XAFS calculations when chemical transferability of a given atomic pair is valid. Since the primary purpose of these standards is to simulate near-neighbor XAFS, multiple scattering is neglected. The ingredients retained in our formulation are summarized below; their order parallels the subroutine calls in the *ab initio* code FEFF. The code is automated such that there are no user-specified parameters in FEFF other than those listed in this paragraph and the optional amplitude and Debye-Waller

factors, thereby ensuring user-independent results.

Atomic Potentials. The atomic potentials and electron densities needed in the construction of the scattering potential are calculated by using the self-consistent, relativistic, Dirac-Fock-Slater atom code of Desclaux,¹⁸ which we have automated for all atoms in the periodic table through americium ($Z \leq 95$). We use the von Barth-Hedin¹⁹ ground-state exchange-correlation potential V_{xc} . For the absorbing atom we impose a *neutral* atomic configuration of a free atom of atomic number $Z_c + 1$ with a missing electron in a given core level, corresponding to the fully relaxed "primary channel".¹⁴ This choice is appropriate for low-energy XAFS and, since the primary channel usually dominates, is a good approximation at high energies as well. Another choice at high energies⁵ is a completely unrelaxed potential, but the differences are usually small. In any case, this choice can also be examined through the use of FEFF by imposing a neutral configuration for a central atom of atomic number Z_c .

Muffin-Tin Potentials. It is especially important for low-energy XAFS calculations to have a good approximation of the molecular potential. Our muffin-tin potential for the absorbing and backscattering atoms is based on the overlapping-atom prescription of Mattheiss²⁰ together with a Norman prescription²¹ for determining muffin-tin radii: the atomic charge densities are overlapped, spherically averaged about each atomic center, and integrated up to the "Norman radius" R_{nm} for which the total electron charge in the sphere is equal to the atomic number Z of the atom. The muffin-tin radii R_{mt} are obtained by proportionately reducing the R_{nm} until the muffin-tins touch. Overlapping muffin-tins and ionized atoms were found to have little effect on the calculated XAFS and are therefore not considered in detail here. The interstitial potential and charge density are determined by a simple averaging of the charge between R_{mt} and R_{nm} for all the atoms, as discussed by Loucks.²² This procedure for calculating interstitial averages is most appropriate for monatomic solids, where the volume of a Norman sphere is the volume per atom, but can overestimate the interstitial charge density in open structures and molecules. The (ground-state) overlapped-atom potential is then given by $V(\vec{r}) = V_{\text{coul}}(\vec{r}) + V_{xc}(\rho(\vec{r}))$, where V_{coul} is the Coulomb potential, V_{xc} the von Barth-Hedin¹⁹ exchange-correlation potential, and ρ the electron charge density. The overlapped-atom approximation is a significant improvement on the renormalized-atom approach used in ref 2, especially for compounds or molecules, and removes the arbitrariness in assigning muffin-tin radii. Note, however, that our model system is constructed with only two atomic species. In cases with more than two species, the construction of an accurate muffin-tin scattering potential can be made with the same procedure, together with a more detailed cluster model.

Energy Reference. Because of the energy dependence of the self-energy, the muffin-tin zero of energy $V_{\text{int}}(E)$ for excited states is also energy dependent, and hence the concept of a precise "inner potential" in XAFS is ambiguous. The variation of $V_{\text{int}}(E)$ over the range of XAFS energies roughly amounts to the magnitude of the exchange hole, i.e., $V_{xc} \sim -k_F/\pi$, in atomic units, where k_F is the Fermi momentum, and is typically about 10 eV (we use atomic units $\hbar = m = e = 1$ for the theoretical formalism in this paper; however, data for the standards are given with distances in angstroms and energies in electronvolts). To circumvent this ambiguity for comparison of our standards with the experimental standards, we have chosen as a fixed energy reference E_0 , the photoabsorption energy threshold. Experimentally this threshold corresponds to an energy near the midpoint of the edge step in the X-ray absorption coefficient. In systems where the Fermi energy corresponds to a bound-state transition, E_0 is identified with the energy of the lowest unbound state. In our calculations the value of E_0 is estimated as the chemical potential μ of a homogeneous electron gas at the average interstitial charge density. From this reference, the photoelectron wavenumber is defined as $k = [2(E - \mu)]^{1/2}$. The errors introduced by the electron-gas approximation, the calculation of interstitial potential and charge density, and the lack of self-consistency in the muffin-tin potential are such that our energy reference is typically a few electronvolts higher than that from self-consistent calculations.^{7,9,10}

Self-Energy. For excited states the exchange-correlation potential $V_{xc}(\rho)$ is replaced by a complex, energy-dependent self-energy $\Sigma(E, \rho)$, based on an analytic fit²³ (which is exact for the imaginary part) to the GW/plasmon-pole self-energy $\Sigma_{\text{HL}}(E, \rho)$ of Hedin and Lundqvist.²⁴ This

(6) Rehr, J. J.; Albers, R. C.; Natoli, C. R.; Stern, E. A. *Phys. Rev. B* **1986**, *34*, 4350. See also: Barton, J. J.; Shirley, D. A. *Phys. Rev. A* **1985**, *32*, 1019. Müller, J. E.; Schaich, W. L. *Phys. Rev. B* **1983**, *27*, 6489. Gurman, S.; Binsted, N.; Ross, I. J. *Phys. C* **1984**, *17*, 143.

(7) Natoli, C. R.; Benfatto, M.; Tyson, T. A.; Hodgson, K. O.; Hedman, B. Stanford University preprint, 1989.

(8) Chou, S.-H.; Rehr, J. J.; Stern, E. A.; Davidson, E. R. *Phys. Rev. B* **1987**, *35*, 2604.

(9) Müller, J. E.; Jepsen, O.; Wilkins, J. W. *Solid State Commun.* **1982**, *42*, 365.

(10) Mustre de Leon, J.; Rehr, J. J.; Zabinsky, S. I.; Albers, R. C. University of Washington preprint, 1991. Mustre de Leon, Jose. Ph.D. Thesis, University of Washington, 1989 (unpublished).

(11) For a recent overview, see: Rehr, J. J. *Physica B: Amsterdam* **1989**, *158*, 1.

(12) Lee, P. A.; Pendry, J. B. *Phys. Rev. B* **1975**, *11*, 2795. See also: Ashley, C. A.; Doniach, S. *Phys. Rev. B* **1975**, *11*, 1279. Schaich, W. L. *Phys. Rev. B* **1973**, *8*, 4028.

(13) Müller, J. E.; Schaich, W. L. *Phys. Rev. B* **1983**, *27*, 6489.

(14) Rehr, J. J.; Stern, E. A.; Martin, R. L.; Davidson, E. R. *Phys. Rev. B* **1978**, *17*, 560.

(15) Lu, D.; Rehr, J. J. *Phys. Rev. B* **1988**, *37*, 6126.

(16) Ekardt, W.; Tran Thoai, D. B. *Solid State Commun.* **1981**, *40*, 939.

(17) Noguera, C.; Spanjaard, D.; Friedel, J. J. *Phys. F: Met. Phys.* **1979**, *9*, 1189.

(18) Desclaux, J. J. *Phys. B* **1971**, *4*, 631; *Comput. Phys. Commun.* **1975**, *9*, 31.

(19) von Barth, U.; Hedin, L. *J. Phys. C* **1972**, *5*, 1629.

(20) Mattheiss, L. *Phys. Rev. A* **1964**, *133*, 1399.

(21) Norman, J. G., Jr. *Mol. Phys.* **1976**, *31*, 1191.

(22) Loucks, T. L. *Augmented Plane Wave Method*; Benjamin: New York, 1967.

(23) Lu, D.; Mustre de Leon, J.; Rehr, J. J. *Physica B* **1989**, *158*, 413.

is nearly equivalent numerically to the self-energy introduced into XAFS theory by Lee and Beni⁵ but is much more efficient computationally. Although there is some evidence for positive corrections to the Hedin-Lundqvist self-energy,¹⁰ it appears to be accurate to within a few electronvolts at XAFS energies. To avoid a discontinuity at $k = 0$, we have defined the self-energy so that the Fermi-level μ is the same for both occupied and excited states, i.e., $\Sigma(E, \rho) = \Sigma_{\text{HL}}(E, \rho) - \Sigma_{\text{HL}}(\mu, \rho) + V_{\text{sc}}(\rho)$. The excited-state potential is therefore given by $V(\vec{r}, E) = V(\vec{r}) + \Sigma_{\text{HL}}(E, \rho(\vec{r})) - \Sigma_{\text{HL}}(\mu, \rho(\vec{r}))$. The advantage of this formulation over other approximations, such as the Dirac-Hara self-energy,⁸ is that extrinsic losses are represented fairly accurately in terms of the imaginary part of $\Sigma(E, \rho)$.

Intrinsic Loss. Because extrinsic and intrinsic losses involve the same final states, interference between these processes must also be considered. We have found¹⁵ that intrinsic losses and interference tend to compensate each other, considerably reducing the net effect of the intrinsic processes alone. Hence for the present, these loss terms are simply lumped into a constant reduction factor S_0^2 , which is typically 0.9. It would be desirable to improve this by an estimate of the energy dependence of this amplitude factor.¹⁵⁻¹⁷

Scattering Potential. The single-scattering XAFS spectrum is calculated from the solution to an electron-atom scattering problem:^{6,12} the unperturbed system contains a photoelectron of energy E and an angular momentum index l moving in a uniform electron gas of charge density ρ_{int} and (lossy) complex potential $V_{\text{int}}(E)$; the perturbation consists of muffin-tin scatterers at the origin (the absorbing atom) and at R (the backscattering atoms). We therefore define the scattering potential for each atom with respect to the energy-dependent muffin-tin zero, i.e., $v(|\vec{r}-\vec{R}|, E) = V(\vec{r}, E) - V_{\text{int}}(E)$, which vanishes outside the muffin-tins. This is one of the main differences between our treatment and that of ref 2, which uses a real muffin-tin zero. With V_{int} as an energy reference, the inelastic loss in a system is mostly accounted for by the uniform mean-free path term. Moreover, since there is no loss in $V(\vec{r}, E)$ in the high-density core region of atoms, the scattering potential $v(r, E)$ is actually amplifying in the core region and hence leads to increases in the backscattering amplitudes and phases compared to those of Lee and Beni,⁵ as noted by Ekardt and Tran Thoai.²⁵

Partial-Wave Phase Shifts. Up to 20 complex partial-wave phase shifts $\delta_l(E)$ are used in the calculations to achieve convergence for all k up to 20 \AA^{-1} . They are obtained by solving the Dirac equation with the complex scattering potential $v(r, E)$ and using an algorithm described by Loucks;²² i.e., solutions to the Dirac equation are matched to free (decaying) spherical waves at energy E propagating in the (complex) interstitial potential $V_{\text{int}}(E)$ beyond the muffin-tin radius. The use of complex phase shifts in our approach results in an energy-dependent enhancement factor $\exp(-\text{Im}(\delta_l))$, in addition to the mean-free path term of other treatments; the factor is enhancing because v is amplifying in the core region, as discussed in the preceding paragraph.

XAFS Spectra. Single-scattering contributions to XAFS spectrum χ_l for a given atom pair and absorption shell are calculated in terms of an exact, curved-wave, effective scattering amplitude.^{6,10} For K-shell XAFS, for example, the curved-wave backscattering amplitude is given by

$$\hat{f}(\pi, p, R) = \frac{1}{p} \sum_l (-1)^l t_l [(l+1)c_{l+1}(pR)^2 + l c_{l-1}(pR)^2] \quad (1)$$

Formulas for other shells are given by Schaich.²⁶ Here $p = [2(E - V_{\text{int}}(E) + i\Gamma/2)]^{1/2}$ is the (complex) photoelectron momentum, $c_l(pR)$ is the polynomial coefficient of the momentum Hankel function $h_l = i^{-l}(e^{ipR}/pR)c_l(pR)$, and $t_l = (e^{2i\delta_l} - 1)/2i$ is the dimensionless diagonal t -matrix element. In the definition of p , Γ is the full line width of the core-hole state; values of Γ for each element are built into FEFF from tabulated values.²⁷ Although \hat{f} is defined in terms of the photoelectron momentum p , the energy dependence of the muffin-tin zero makes this definition ambiguous for comparison with experimental results. However, by the replacement $\hat{f} \rightarrow (p/k) \exp[i2(k-p)R] f_{\text{eff}}$, the full spectrum can be recast in standard form¹⁰ and expressed as a function of the photoelectron wavenumber measured from threshold, $k = [2(E - E_0)]^{1/2}$

$$\chi_l^{(1)}(E) = -N A(E) \frac{|f_{\text{eff}}(\pi, k, R)|}{kR^2} \sin(2kR + 2\delta_c + \Phi) e^{-2R/\lambda} e^{-2\sigma^2 k^2} \quad (2)$$

Here, $f_{\text{eff}}(\pi, k, R) = |f_{\text{eff}}(\pi, k, R)| e^{i\Phi}$ is the effective curved-wave scattering amplitude, δ_c is the real part of the final-state l -wave central-atom phase

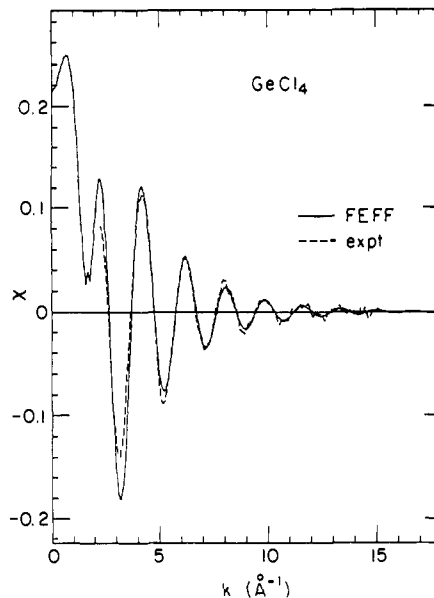


Figure 1. XAFS spectrum $\chi(k)$ for GeCl_4 from FEFF (solid line) as calculated with the parameters in Table I and from unfiltered experimental data²⁹ (dashed line).

Table I. Parameters Used in ab Initio Calculations

	$R, \text{ \AA}$	S_0^2	$\sigma^2, \text{ \AA}^2$	$\sigma_{\text{mm}}^2, \text{ \AA}^2$	$\delta R, \text{ \AA}$	$\delta \sigma^2, \text{ \AA}^2$
GeCl_4	2.110	1.08	0.00212	0.00032	0.002	0.0007
Cu	2.552	0.85	0.00530	0.00052	0.018	0.0002
Pt	2.772	0.89	0.00321	0.00040	0.002	0.0004

shift, $\lambda = 1/(\text{Im}(p))$ is the XAFS mean-free path, σ is the rms fluctuation in the bond length R , and $A(E) = S_0^2(E) \exp[-\text{Im}(\delta_c(E))]$ is a factor that combines intrinsic losses, final-state interference effects, and central-atom losses.

III. Ab initio XAFS Standards

The fully automated computer code, FEFF, which is based on the above theoretical model, makes possible calculations of ab initio XAFS standards.²⁸ They have a significant advantage over tabulated standards in that the assumption of chemical transferability is not usually imposed. Indeed, FEFF constructs a standard tailored to a particular chemical environment. This is particularly important for compound structures, for both the shape of the XAFS spectrum and the location of the zero of energy.¹⁰ It was for this reason that the renormalized-atom prescription had to be abandoned in favor of the overlapping-atom potential presently used. In cases with more than two atomic species in the first coordination shell, the description of the chemical environment with our model system will be less accurate. In such cases FEFF can still be used to obtain the XAFS for a given atomic pair, but the validity of the results will depend on the validity of transferability, albeit a weaker form of transferability than that for atoms.

The theoretical data for each XAFS standard consist of the normalized XAFS spectrum $\chi_l(k)$ on a uniform grid of 400 k points between 0 and 20 \AA^{-1} , simulating experimental data. In addition, we tabulate on the same grid the amplitude $|\chi_l(k)|$ and the total XAFS phase $(2\delta_c + \Phi)$ and over a 49-point grid the more smoothly varying XAFS phases and amplitudes in eq 2, namely $2\delta_c$, $|f_{\text{eff}}|$, Φ , $A(E)$, and λ as well as the real part of p . A typical standard spectrum, namely that for the GeCl_4 molecule, is shown in Figure 1, together with the experimental XAFS.²⁹ The parameters in our calculations are listed in Table I. Our results for χ are in good agreement with the self-consistent calculations of Natoli et al.⁷

(24) Hedin, L.; Lundqvist, S. *Solid State Phys.* **1969**, *23*, 1. Lundqvist, B. I. *Phys. Condens. Matter* **1977**, *6*, 206.

(25) Ekardt, W.; Tran Thoai, D. B. *Solid State Commun.* **1981**, *40*, 939.

(26) Schaich, W. L. *Phys. Rev. B* **1984**, *29*, 6513.

(27) Rahnkonen, K.; Krause, K. *At. Data Nucl. Data Tables* **1974**, *14-2*, 140.

(28) Those interested obtaining the ab initio FEFF codes or the FEFF tables should contact the authors.

(29) Bouldin, C. E.; Bunker, G. B.; McKeown, D. A.; Forman, R. A.; Ritter, J. J. *Phys. Rev. B* **1988**, *38*, 10816.

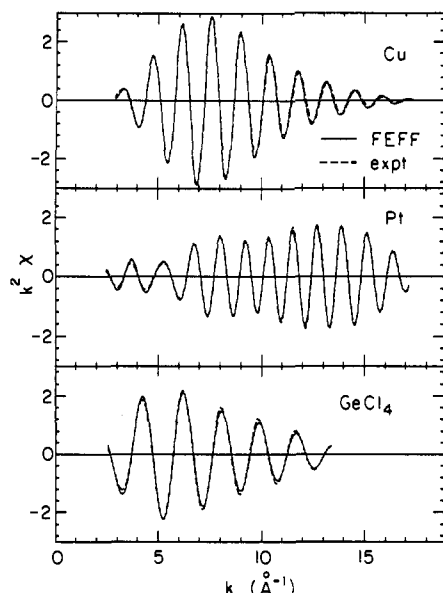


Figure 2. Filtered XAFS data $k^2\chi(k)$ for the first coordination shell of Cu, Pt, and GeCl_4 from FEFF (solid lines) and from similarly filtered experimental data^{29,30} (dashed lines).

A quantitative comparison between single-scattering theory and experimental results requires Fourier filtering or fitting to eliminate multiple-scattering terms in the experimental spectrum. Indeed, since the primary utility of XAFS analysis is the determination of nearest-neighbor distance and coordination numbers, we shall focus our discussion below on the filtered first-shell results. Thus in Figure 2 we present the Fourier-filtered XAFS standards for Cu, Pt, and GeCl_4 , together with similarly filtered K-shell experimental data for Cu at 190 K,³⁰ LIII-shell Pt at 190 K,³⁰ and K-shell GeCl_4 at 300 K,²⁹ in which only the first near-neighbor contribution to χ is retained. The parameters used in these calculations are listed in Table I. In all cases the known Debye-Waller factor³¹ was imposed. In addition, a "McMaster correction factor" was added to correct for the edge-step normalization of the XAFS used in refs 29 and 30; i.e., the theoretical spectrum $\chi = [\mu - \mu_0(E)]/\Delta\mu_0(E)$ was multiplied by a factor $\Delta\mu_0(E)/\Delta\mu_0 \sim \exp(-\gamma E)$ to correspond to the experimental XAFS, $\chi = [\mu - \mu_0(E)]/\Delta\mu_0$. Here $\mu(E)$ is the X-ray absorption coefficient, $\mu_0(E)$ is the background absorption, $\Delta\mu_0$ is the edge step, and $\Delta\mu_0(E)$ is the difference in extrapolated absorption curves.³² This correction is well represented by a factor $\exp(-2\sigma_{\text{mm}}^2 k^2)$, i.e., by a small positive (about 10%) addition to the thermal σ^2 (see Table I). The only free parameter in our calculations is an overall amplitude factor S_0^2 . We have found that $S_0^2(E)$ can be represented as a phenomenological constant, which is typically 0.9 to within about 20%. This constant is expected to be somewhat larger in molecular systems, where the interstitial charge density (and hence the extrinsic losses) tends to be overestimated by our approximations. Indeed, a value of $S_0^2 \sim 1.08$ is needed for GeCl_4 but only 0.85 for Cu and 0.89 for Pt are needed. In these calculations the energy references μ are -5.51, -3.26, and -2.28 eV for Cu, Pt, and GeCl_4 , respectively; the corresponding ground-state muffin-tin zeros are $V_{\text{in}}(\mu) = -17.8, -17.9,$ and -16.6 eV, and the core-hole lifetimes are $\Gamma = 1.76, 4.82,$ and 2.34 eV. These reference energies are a few electronvolts above the midpoint of the edge step or the Fermi energy of self-consistent calculations.

We feel this degree of accuracy is presently adequate for XAFS analysis but probably not for XANES. Moreover, our reference

(30) Stern, E. A.; Bunker, B. A.; Heald, S. M. *Phys. Rev. B* **1980**, *21*, 5521.

(31) Values of σ^2 for Cu and Pt are given by: Sevillano, E.; Meuth, H.; Rehr, J. J. *Phys. Rev. B* **1979**, *20*, 4908. That for GeCl_4 is given by: Marino, Y.; Nakamura, Y.; Iijima, T. *J. Chem. Phys.* **1960**, *32*, 643.

(32) McMaster, W. H.; Kerr-Del Grande, N.; Mallett, J. H.; Hubbell, J. H. *Compilation of X-ray Cross Sections*. Lawrence Radiation Laboratory Report UCRL-50174; National Bureau of Standards: Springfield, VA, 1969.

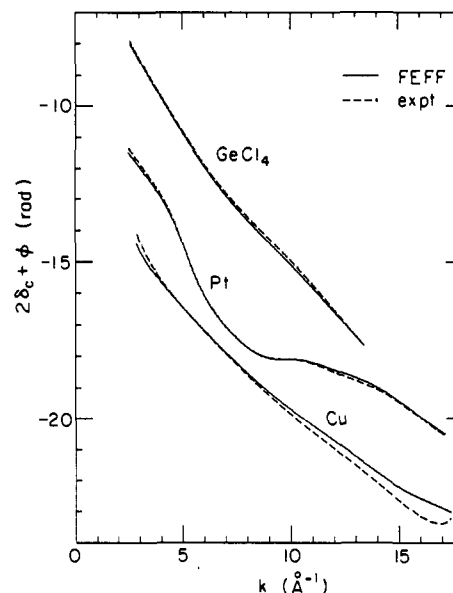


Figure 3. Filtered total XAFS phase ($2\delta_c + \Phi$) for the first coordination shell of Cu, Pt, and GeCl_4 from FEFF (solid lines) and from similarly filtered experimental data^{30,29} (dashed lines).

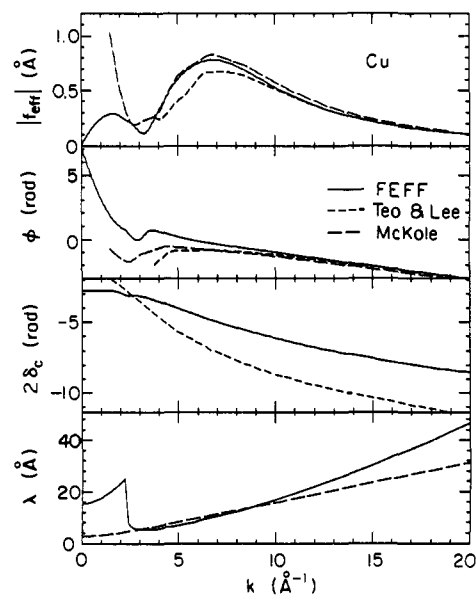


Figure 4. XAFS phases and amplitudes in the XAFS equation (2) for Cu from FEFF (solid lines) and from the tables of Teo and Lee² (short dashes) and McKale et al.³ (long dashes): top panel, magnitude of the back-scattering amplitude $|f_{\text{eff}}|$; second panel, phase of the backscattering amplitude Φ ; third panel, central-atom phase shift $2\delta_c$; fourth panel, mean-free path λ (solid line). For comparison the mean-free path for a constant imaginary potential of 5 eV is also shown (long dashes).

provides an unambiguous way of estimating the experimental value of E_0 , accurate to a few electronvolts: by alignment of the low-energy peaks and nodes in the experimental XAFS to the theoretical standards, E_0 is given by the experimental energy corresponding to $k = 0$. The agreement between theoretical and experimental XAFS spectra is very good over the full range of the background-subtracted experimental data, typically $k = 2$ – 17 \AA^{-1} . Figure 3 shows that the agreement between the calculated and measured total XAFS phases ($2\delta_c + \Phi$) is also very good. For Pt, the agreement in phase is significantly better than that reported by Teo and Lee² and is maintained over a more extended range. The overall agreement in the XAFS amplitude is also better, especially at low wavenumbers. Discrepancies in estimates of R and σ^2 are also given in Table I. In all cases, they are smaller than 0.02 \AA , but we do not understand why some comparisons are better than others. The discrepancy for Cu also exceeds 0.015 \AA in previous studies.^{2,3} A comparison of the overall goodness

Table II. XAFS Parameters from FEFF for K-Shell Cu at $R = 2.552 \text{ \AA}$

$k, \text{ \AA}^{-1}$	$\text{Re}(2\delta_c), \text{ rad}$	$f_{\text{eff}}, \text{ \AA}$	$\Phi, \text{ rad}$	$A(E)$	$\lambda, \text{ \AA}$	$\text{Re}(p), \text{ \AA}$
2.0	3.349	0.277	-11.5	1.012	23.48	2.71
4.0	2.729	0.319	-11.9	1.217	5.79	4.31
6.0	1.759	0.744	-12.7	1.031	8.59	6.15
10.0	0.147	0.534	-13.5	0.924	16.89	10.06
20.0	-2.234	0.106	-15.6	0.876	46.57	20.02

Table III. XAFS Parameters from FEFF Tables for K-Shell Cu at $R = 2.0 \text{ \AA}$ (Upper) and at $R = 3.0 \text{ \AA}$ (Lower)

$k, \text{ \AA}^{-1}$	$\text{Re}(2\delta_c), \text{ rad}$	$f_{\text{eff}}, \text{ \AA}$	$\Phi, \text{ rad}$	$A(E)$	$\lambda, \text{ \AA}$	$\text{Re}(p), \text{ \AA}$
2.0	3.349	0.177	-12.1	1.012	23.47	2.71
4.0	2.730	0.377	-11.8	1.217	5.79	4.31
6.0	1.760	0.751	-12.7	1.031	8.59	6.15
10.0	0.147	0.520	-13.5	0.924	16.90	10.06
20.0	-2.234	0.107	-15.6	0.875	46.58	20.02
2.0	3.349	0.322	-11.0	1.012	23.47	2.71
4.0	2.730	0.299	-11.9	1.217	5.79	4.31
6.0	1.760	0.738	-12.6	1.031	8.59	6.15
10.0	0.147	0.542	-13.5	0.924	16.90	10.06
20.0	-2.234	0.108	-15.5	0.875	46.58	20.02

of fit between theory and experiment on well characterized materials for which excellent experimental data are available, namely K-shell Cu and Rh and L_{III}-shell Pt, showed that the ab initio FEFF standards yield significantly better fits to XAFS amplitudes and phases than other methods.³³

Figure 4 shows the decomposition of the XAFS spectrum for Cu into its component phases and amplitudes. Sample entries of the tabulated data from FEFF at $k = 2, 4, 6, 10,$ and 20 \AA^{-1} are given in Table II. For comparison, results from the tables of Teo and Lee² and McKale et al.³ are also shown in Figure 4. Because of differences in our theoretical formulation, our phases and amplitudes bear only semiquantitative resemblance to those results. These differences are due to the different ways curved-wave effects, inelastic losses, and the energy reference are treated.^{10,25} We also show in Figure 4 (fourth panel) the mean-free path calculated by FEFF. The structure at very low k is an artifact of plasmon excitations in our model self-energy. The McKale tables and EXCURV require a mean-free path to be added as a constant imaginary potential. Such an approximation is also shown in Figure 4 (fourth panel) and observed to be reasonably accurate over a wide energy range. Additional comparisons between theory and experiment are given in ref 10.

IV. Tabulated XAFS Standards

To the extent that chemical effects are negligible, tables of XAFS parameters may be adequate for the analysis of XAFS experiments. Using FEFF, we have constructed such tables for all elements in the periodic table through $Z = 94$ for both K ($Z \leq 50$) and L_{III} ($40 \leq Z \leq 94$) shells. For each element, an appropriate standard scattering potential is obtained by assuming a monatomic solid at a physical near-neighbor distance R_0 and an appropriate coordination number, again by using the overlapped-atom prescription described in section II. The table construction required about 3 CPU h on a Sun 4/60 workstation, and all the data can be stored on a single 1.2-MB floppy diskette. Near-neighbor distances R in $f_{\text{eff}}(\pi, k, R)$ were fixed arbitrarily at typical values, namely 2.0 and 3.0 \AA . Data for other distances and wavenumbers may be obtained by interpolation⁶ (or extrapolation) in $1/R$ and k . Each table contains data for 49 points between $k = 0$ (i.e., $p = k_F$) and $k = 20 \text{ \AA}^{-1}$. Sample data for Cu at selected wavenumbers ($k = 2, 4, 6, 10,$ and 20 \AA^{-1}) are given in Table III.

As noted above, these results differ noticeably from previous tables.^{2,3} However, all tables use the Hedin-Lundqvist self-energy for the central-atom phase shift (McKale et al.³ do not present

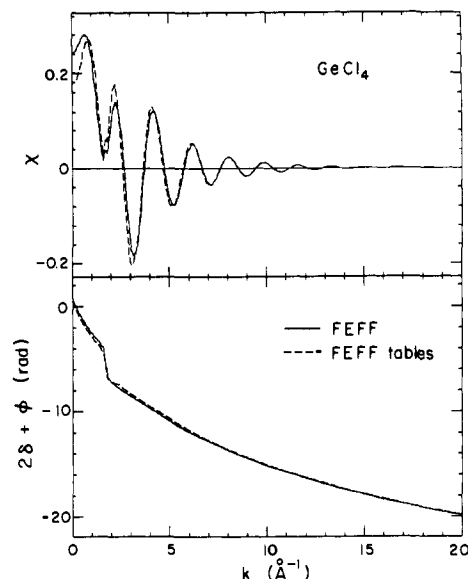


Figure 5. XAFS spectrum for GeCl_4 from FEFF (solid lines) and from interpolated FEFF tables for Ge and Cl at $R = 2.11 \text{ \AA}$ (short dashes): top panel, $\chi(k)$; lower panel, total XAFS phase ($2\delta_c + \Phi$).

Table IV. XAFS Parameters from FEFF for GeCl_4 at $R = 2.11 \text{ \AA}$ (Upper) and from Interpolated FEFF Tables for a Ge Central Atom and a Cl Backscatterer (Lower)

$k, \text{ \AA}^{-1}$	$\text{Re}(2\delta_c), \text{ rad}$	$f_{\text{eff}}, \text{ \AA}$	$\Phi, \text{ rad}$	$A(E)$	$\lambda, \text{ \AA}$	$\text{Re}(p), \text{ \AA}$
2.0	4.730	0.256	-11.9	1.114	18.20	2.79
4.0	3.728	1.029	-13.5	1.371	5.43	4.38
6.0	2.694	0.675	-14.6	1.142	7.77	6.19
10.0	0.982	0.252	-16.1	1.033	14.94	10.00
20.0	-1.568	0.049	-18.3	0.974	40.22	20.00
2.0	4.765	0.322	-11.8	1.120	46.60	2.77
4.0	3.802	1.022	-13.3	1.342	5.91	4.35
6.0	2.777	0.683	-14.5	1.123	8.54	6.18
10.0	1.009	0.262	-16.0	1.017	16.74	10.08
20.0	-1.560	0.051	-18.3	0.959	46.91	20.03

central-atom phase shifts based on their ground-state X_α potential; rather they simply borrow those from the Teo and Lee tables). We believe the reason that all tables give fairly accurate distance estimates in XAFS studies is that the Hedin-Lundqvist self-energy is an adequate approximation for calculating the central-atom phase shift, a quantity which dominates the total XAFS phase.

By comparing the ab initio and tabulated standards, we can obtain a theoretical test of chemical transferability in XAFS. If transferability is valid, the results from FEFF and from the FEFF tables should agree. Consider, for example, the XAFS of GeCl_4 with a K-shell Ge central atom and a Cl backscatterer. Figure 5 gives the XAFS spectrum both from FEFF and from the corresponding FEFF tables by interpolation in $1/R$ at $R = 2.11 \text{ \AA}$. This is a favorable case for transferability, as the molecule is 80% Cl, and the results are in good agreement in the EXAFS regime, although chemical effects are observable below 4 \AA^{-1} . Selected entries from the XAFS amplitude and phase tables generated by FEFF and by interpolation from the FEFF tables are in Table IV. These results indicate that chemical transferability is a good approximation for GeCl_4 , especially above $k = 5 \text{ \AA}^{-1}$. Indeed, XAFS analysis of these results indicates that the shift in near-neighbor distance from the tabulated data is less than 0.01 \AA . If only low-wavenumber data were available, e.g., in the case of large disorder or low- Z scatterers, the tabulated standards would be less adequate. A comparison of the XAFS for the C-C bond in C_2H_6 , for example, showed that transferability is again a reasonable approximation above $k = 5 \text{ \AA}^{-1}$; however, the XAFS data does not extend much beyond $k = 10 \text{ \AA}^{-1}$. For these reasons tabulated standards should generally be used with caution. In any case, the ab initio standards permit a check on the validity of transferability case by case.

(33) Vaarkamp, M.; Königsberger, D. In *XAFS VI: Proceedings of the Sixth International Conference on XAFS and Near Edge Structure*; Hasnain, S., Ed.; Ellis Horwood Ltd.: Chichester, U.K., 1990.

V. Summary and Conclusions

We have derived new theoretical XAFS standards based on an *ab initio* code FEFF, which yield simulated XAFS spectra $\chi(k)$ together with the phase shifts and scattering amplitudes that appear in the standard XAFS equation, eq 2. We have shown that an unambiguous "inner potential" cannot be defined in XAFS, with the consequence that these amplitudes and phases are *not* the same as those of other treatments.^{2,3} The standards are of two types: *ab initio standards* that give the XAFS for a particular atom pair and *tabulated standards* that are based on individual atomic potentials. These standards have several advantages compared with previous formulations: (a) compared to the case of studies that use tables, the assumption of chemical transferability is usually not required in the *ab initio standards*; (b) unlike other *ab initio* codes, FEFF requires as input parameters only atomic numbers, coordination numbers, and the near-neighbor distance; there are no user-adjustable parameters other than the usual amplitude and Debye–Waller factors, making the code extremely easy to run and ensuring user-independent results; (c) unlike published tables, FEFF can be modified to incorporate improvements to the theoretical model; (d) the codes can be extended for other spectroscopies, e.g., photoelectron diffraction;^{34,35} and (e) the standards provide a theoretical test of the chemical transferability hypothesis. We have attempted to remove the "black box" aspect of *ab initio* codes, such as EXCURV, by tabulating all the ingredients in the standard XAFS formula, i.e., the amplitudes, phase shifts, and loss terms in eq 2, not just the overall XAFS spectrum. Moreover, we also determine the energy reference E_0 to within a few electronvolts. The FEFF tables provide curved-wave XAFS amplitudes and phases over a wider range for all $Z \leq 94$ and thus supplant existing tabulations. While less reliable than individual calculations, the tables yield good approximations for XAFS phases and amplitudes for nearest neighbors in the EXAFS range as well as quick estimates of more distant neighbor contributions to XAFS.

In deriving these new XAFS standards, we have endeavored to extend the theory to lower wavenumbers and remove the limitations of previous formulations such as the need for ad hoc parameters. However, the theory is probably unreliable within 10 eV of the absorption edge (i.e., $k < 2 \text{ \AA}^{-1}$). Independent tests on Cu, Rh, and Pt have verified that FEFF gives more accurate XAFS simulations over a wider range, for both amplitude and phase, than other methods.³³ A significant innovation, we feel,

is our efficient treatment of the Hedin–Lundqvist self-energy $\Sigma_{\text{HL}}(E)$, which permits *ab initio* calculations in CPU minutes on modern PC's and workstations. The use of ground-state exchange-correlation potentials such as the X_α potential leads to significant phase and amplitude errors that cannot be compensated with an energy shift. An adequate molecular potential based on relativistic atomic potentials is found to be essential for an accurate description of XAFS phases and amplitudes. Our overlapped-atom prescription is found to yield results for XAFS spectra comparable to those from self-consistent codes. Our approximation does, however, tend to overestimate the energy threshold and inelastic losses, especially in molecules, and should be improved for XANES studies. Recently FEFF has been extended²⁸ to accommodate single-scattering XAFS contributions from a multishell cluster containing several atomic species. This improvement permits one to assess the validity of the *ab initio* standards in complex systems, for example, cases where the first coordination shell contains more than one type of atom or where there is substantial interference between first and second shells. Tests using the multishell code indicate that the FEFF standards appear to be reliable in such systems. This indicates that the local coordination numbers are important in obtaining transferable XAFS standards. Other desirable improvements to the code include polarization dependence, better treatments of intrinsic losses, the addition of dipole-matrix elements, and a provision for calculating multiple-scattering contributions.^{35,36}

We feel that these new standards are comparable in quality to experimental standards, permitting distance estimates to 0.02 \AA , coordination number determinations to within 20%, Debye–Waller factors to within 20%, and a better overall fit of experimental spectra beyond about 10 eV above the edge (i.e., $k > 2 \text{ \AA}^{-1}$). While less reliable than the *ab initio* standards, the new tabulated standards appear to be adequate for experimental analysis in the EXAFS regime, i.e., typically above $k = 5 \text{ \AA}^{-1}$.

Acknowledgment. We wish to thank J. Alben, M. Benfatto, C. Bouldin, B. Bunker, S. Cramer, A. Djaoui, R. Felton, D. Königsberger, M. Marcus, C. R. Natoli, E. A. Stern, T. Tyson, D. Sayers, and other users of FEFF for valuable comments and suggestions. We thank the NSLS and the X-11 PRT at Brookhaven National Laboratory for hospitality and support in the development of a preliminary version of FEFF. This work was supported in part by DOE Grant DE-FG06-90ER45415 (J.J.R.).

Registry No. GeCl₄, 10038-98-9; Cu, 7440-50-8; Pt, 7440-06-4.

(34) Rehr, J. J.; Albers, R. C. *Phys. Rev. B* **1990**, *41*, 8139.

(35) Mustre de Leon, J.; Rehr, J. J.; Natoli, C. R.; Fadley, C. S.; Osterwalder, J. *Phys. Rev. B* **1990**, *39*, 5632. Yang, A. B.; Brown, F. C.; Rehr, J. J.; Mustre de Leon, J.; Mason, M. G.; Tan, Y. *Bull. Am. Phys. Soc.* **1989**, *35*, 790.

(36) Gurman, S. J.; Binsted, N.; Ross, I. *J. Phys. C* **1986**, *19*, 1845. Natoli, C. R.; Benfatto, M.; Doniach, S. *Phys. Rev. A* **1986**, *34*, 4682. Natoli, C. R.; Benfatto, M. *J. Phys., Colloque* **1986**, No. 8, 11. Vvedensky, D. D.; Saldin, D. K.; Pendry, J. B. *Comput. Phys. Commun.* **1986**, *40*, 421.